A&A 366, 1003–1007 (2001)
DOI: 10.1051/0004-6361:20000331

Astronomy & Astrophysics

High resolution spectroscopy over 8500–8750 Å for GAIA*,**,***

III. A library of synthetic spectra for 7750$\leq T_{\rm eff} \leq$ 50 000 K

F. Castelli[1] and U. Munari[2,3]

[1] CNR-GNA-Osservatorio Astronomico di Trieste Via Tiepolo 11, 34131 Trieste, Italy
[2] Osservatorio Astronomico di Padova, Sede di Asiago, 36012 Asiago (VI), Italy
[3] Centro Interpardimentale Studi ed Attività Spaziali (CISAS "G. Colombo"), Università di Padova, Italy

Received 8 September 2000 / Accepted 23 November 2000

Abstract. In this paper we complete the library of synthetic spectra for the range 7650–8750 Å, which includes the 8500–8750 Å interval currently base-lined for the spectroscopic observations by GAIA, candidate ESA Cornerstone 5 mission. As for Paper II, the spectra are based on Kurucz's codes and line data. The explored metallicity, gravity and temperature ranges are $-2.5 \leq [Z/Z_\odot] \leq +0.5$, $4.5 \leq \log g \leq 2.0$ and 7750 $\leq T_{\rm eff} \leq$ 50 000 K, respectively. The 698 new spectra are computed at the same $\lambda/\triangle\lambda = 20\,000$ resolving power of the observed spectra given in Paper I (131 standard stars mapping the MKK spectral classification system) and the 254 synthetic spectra of Paper II (characterized by $T_{\rm eff} \leq 7\,500$ K).

Key words. atlases – surveys – stars: fundamental parameters

1. Introduction

GAIA is the approved ESA Cornerstone 6 mission designed to obtain extremely precise astrometry (in the *micro*-arcsec regime), multi-band photometry and medium/high resolution spectroscopy for a large sample of stars. The goals as depicted in the mission *Red Book* (ESA SP-2000-4) call for astrometry and broad band photometry to be collected for all stars down to $V \sim 20$ mag over the entire sky ($\sim$1 10^9 stars), with brighter magnitude limits for spectroscopy and intermediate band photometry. Each target star should be measured over a hundred times during the five year mission life-time, in a fashion similar to the highly successful *Hipparcos* operational mode. The astrophysical guidelines of the GAIA mission are discussed by Gilmore et al. (1998) and Perryman (1999), an overview of the GAIA payload and spacecraft is presented by Mérat et al. (1999), and the goals of the GAIA spectroscopy and the merits of the 8500–8750 Å region are discussed by Munari (1999).

This third paper completes the establishment of a data-bank of input data for simulations and evaluation of GAIA spectroscopic performances. As for the whole series, the results are also of general interest to ground-based spectroscopists working at moderately high resolving powers in the near-IR region of the spectrum. Throughout this series a constant resolving power $R = \lambda/\triangle\lambda = 20\,000$ has been maintained. This is at the higher end of the range of dispersions currently considered for implementation on GAIA (between 0.25 and 1.00 Å/pix). Observing and computing at the highest resolution leaves unaltered the possibilities to degrade the results to a lower resolution as later possibly required, while the contrary is not feasible.

In Paper I (Munari & Tomasella 1999) we have built up a homogeneous observational data-bank composed by the spectra of 131 standard stars mapping the MKK classification system from types O4 to M8 and luminosity classes from I to V. In Paper II (Munari & Castelli 2000) we presented a library of 254 synthetic spectra covering the part of the $[Z/Z_\odot]$, log g and $T_{\rm eff}$ space where the vast majority of GAIA targets will be located. They are F-G-K-M type stars with metallicities ranging from those of the galactic globular clusters to that of the Pop. I objects and thus the spectral grid extended over $-2.5 \leq [Z/Z_\odot] \leq +0.5$, $4.5 \leq \log g \leq 1.0$ and

Send offprint requests to: U. Munari,
e-mail: `munari@pd.astro.it`

* Tables 2–4 are only available in electronic form at the CDS via anonymous ftp to `cdsarc.u-strasbg.fr (130.79.128.5)` or via
`http://cdsweb.u-strasbg.fr/cgi-bin/qcat?J/A+A/366/1003`
or via the personal HomePage
`http://ulisse.pd.astro.it/Astro/Atlases/`

** The spectra are available in electronic form at the CDS.

*** Figures 5–224 are only available in electronic form at `http://www.edpsciences.org`

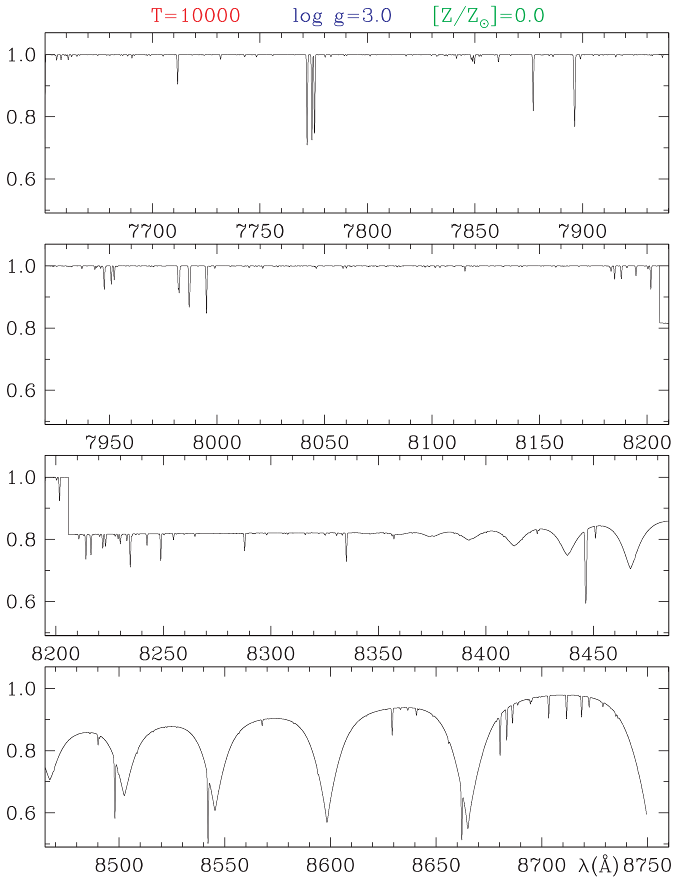

Fig. 1. All spectra have been computed over a range wider that the 8500–8750 Å considered in this series of papers. This plot shows the full explored range (7650–8750 Å)

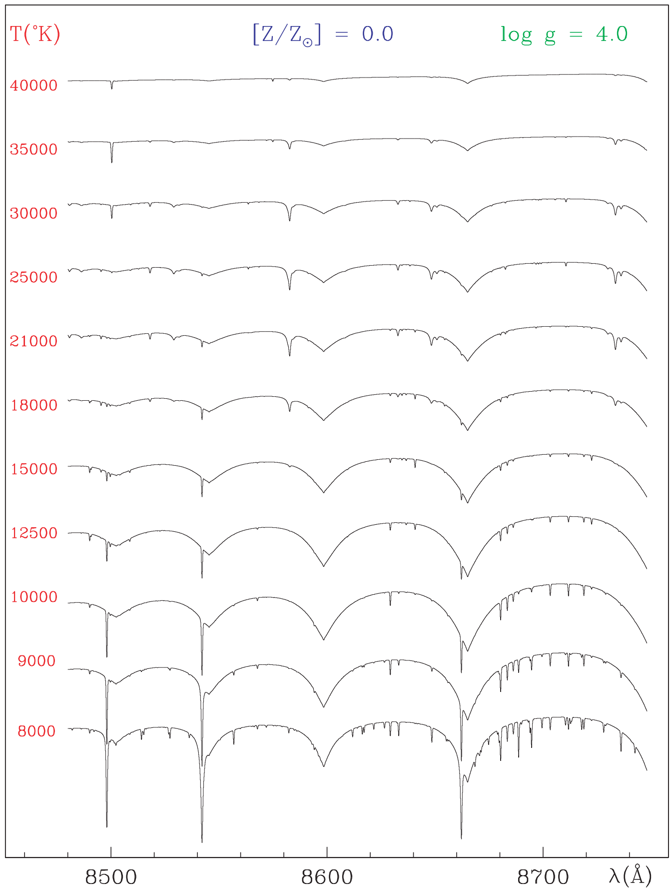

Fig. 2. A sample of $[Z/Z_{\odot}] = 0.0$ synthetic spectra arranged in a sequence showing the effect of varying the temperature

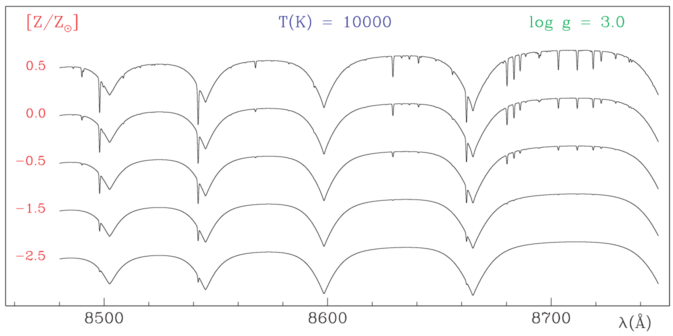

Fig. 3. A sample of $T_{\rm eff}$ = 10 000 K, log g = 3.0 synthetic spectra arranged in a sequence showing the effect of varying the metallicity

$T_{\rm eff}$ $\leq$ 7500 K. The present Paper III completes the spectral mapping toward the higher temperatures (covering A, B and O type stars) by presenting 698 new spectra in the 7750 K $\leq T_{\rm eff}$ $\leq$ 50 000 K temperature range.

2. The synthetic spectra

The grid of 698 computed synthetic spectra is listed in Table 1 where the number of the electronic figure containing the spectra is given. In fact, for each $T_{\rm eff}$, $[Z/Z_{\odot}]$ pair, there is a figure which displays spectra for different surface gravities which roughly correspond to luminosity classes V, III, and I in the MKK classification system. Only the pair of spectra corresponding to $T_{\rm eff}$ = 32 000 K, $[Z/Z_{\odot}]$ = +0.5, log g = 3.25 and $T_{\rm eff}$ = 40 000 K, $[Z/Z_{\odot}]$ = +0.5, log g = 4.0 are missing in this scheme (cf. Table 1 and Figs. 214 and 224), because no radiative equilibrium for the upper layers of the two models was ever achieved in the computations.

The spectra for the whole 7650–8750 Å interval (including the spectra of Paper I and Paper II) are available in electronic ASCII form at the CDS. An example of computed spectrum normalized to the continuum level for the full 7650–8750 Å interval and $T_{\rm eff}$ = 10 000 K, $[Z/Z_{\odot}]$ = 0.0, log g = 3.0 parameters is presented in Fig. 1. All the other Figs. 2–224 show the computed spectrum normalized to the continuum level focusing on the GAIA 8500–8750 Å interval only. To avoid over-crowding in Figs. 220–224, the spectra with $T_{\rm eff}$ = 37 500 K, log g = 4.5 and $T_{\rm eff}$ = 34 000 K, log g = 4.5 are not plotted.

The effects caused by changing the temperature, the metallicity and the gravity in a few example cases are illustrated in Figs. 2, 3 and 4 respectively. Figure 4 is a template for the Figs. 5–224 only available in electronic form.

Table 1. The Metallicity-Temperature-Gravity grid mapped by our synthetic spectra. The numbers-in-the-boxes give the corresponding electronic figure where the given triplet of spectra is plotted. For the numbers in bracketts see text, Sect. 2

	[$Z/Z_\odot$]	T	*log g*		[$Z/Z_\odot$]	T	*log g*		[$Z/Z_\odot$]	T	*log g*		[$Z/Z_\odot$]	T	*log g*		[$Z/Z_\odot$]	T	*log g*
	–2.5	7750	2.0		–1.5	7750	2.0		–0.5	7750	2.0		0.0	7750	2.0		+0.5	7750	2.0
05	–2.5	7750	3.0	**06**	–1.5	7750	3.0	**07**	–0.5	7750	3.0	**08**	0.0	7750	3.0	**09**	+0.5	7750	3.0
	–2.5	7750	4.0		–1.5	7750	4.0		–0.5	7750	4.0		0.0	7750	4.0		+0.5	7750	4.0
	–2.5	8000	2.0		–1.5	8000	2.0		–0.5	8000	2.0		0.0	8000	2.0		+0.5	8000	2.0
10	–2.5	8000	3.0	**11**	–1.5	8000	3.0	**12**	–0.5	8000	3.0	**13**	0.0	8000	3.0	**14**	+0.5	8000	3.0
	–2.5	8000	4.0		–1.5	8000	4.0		–0.5	8000	4.0		0.0	8000	4.0		+0.5	8000	4.0
	–2.5	8250	2.0		–1.5	8250	2.0		–0.5	8250	2.0		0.0	8250	2.0		+0.5	8250	2.0
15	–2.5	8250	3.0	**16**	–1.5	8250	3.0	**17**	–0.5	8250	3.0	**18**	0.0	8250	3.0	**19**	+0.5	8250	3.0
	–2.5	8250	4.0		–1.5	8250	4.0		–0.5	8250	4.0		0.0	8250	4.0		+0.5	8250	4.0
	–2.5	8500	2.0		–1.5	8500	2.0		–0.5	8500	2.0		0.0	8500	2.0		+0.5	8500	2.0
20	–2.5	8500	3.0	**21**	–1.5	8500	3.0	**22**	–0.5	8500	3.0	**23**	0.0	8500	3.0	**24**	+0.5	8500	3.0
	–2.5	8500	4.0		–1.5	8500	4.0		–0.5	8500	4.0		0.0	8500	4.0		+0.5	8500	4.0
	–2.5	8750	2.0		–1.5	8750	2.0		–0.5	8750	2.0		0.0	8750	2.0		+0.5	8750	2.0
25	–2.5	8750	3.0	**26**	–1.5	8750	3.0	**27**	–0.5	8750	3.0	**28**	0.0	8750	3.0	**29**	+0.5	8750	3.0
	–2.5	8750	4.0		–1.5	8750	4.0		–0.5	8750	4.0		0.0	8750	4.0		+0.5	8750	4.0
	–2.5	9000	2.0		–1.5	9000	2.0		–0.5	9000	2.0		0.0	9000	2.0		+0.5	9000	2.0
30	–2.5	9000	3.0	**31**	–1.5	9000	3.0	**32**	–0.5	9000	3.0	**33**	0.0	9000	3.0	**34**	+0.5	9000	3.0
	–2.5	9000	4.0		–1.5	9000	4.0		–0.5	9000	4.0		0.0	9000	4.0		+0.5	9000	4.0
	–2.5	9250	2.0		–1.5	9250	2.0		–0.5	9250	2.0		0.0	9250	2.0		+0.5	9250	2.0
35	–2.5	9250	3.0	**36**	–1.5	9250	3.0	**37**	–0.5	9250	3.0	**38**	0.0	9250	3.0	**39**	+0.5	9250	3.0
	–2.5	9250	4.0		–1.5	9250	4.0		–0.5	9250	4.0		0.0	9250	4.0		+0.5	9250	4.0
	–2.5	9500	2.0		–1.5	9500	2.0		–0.5	9500	2.0		0.0	9500	2.0		+0.5	9500	2.0
40	–2.5	9500	3.0	**41**	–1.5	9500	3.0	**42**	–0.5	9500	3.0	**43**	0.0	9500	3.0	**44**	+0.5	9500	3.0
	–2.5	9500	4.0		–1.5	9500	4.0		–0.5	9500	4.0		0.0	9500	4.0		+0.5	9500	4.0
	–2.5	9750	2.0		–1.5	9750	2.0		–0.5	9750	2.0		0.0	9750	2.0		+0.5	9750	2.0
45	–2.5	9750	3.0	**46**	–1.5	9750	3.0	**47**	–0.5	9750	3.0	**48**	0.0	9750	3.0	**49**	+0.5	9750	3.0
	–2.5	9750	4.0		–1.5	9750	4.0		–0.5	9750	4.0		0.0	9750	4.0		+0.5	9750	4.0
	–2.5	10000	2.0		–1.5	10000	2.0		–0.5	10000	2.0		0.0	10000	2.0		+0.5	10000	2.0
50	–2.5	10000	3.0	**51**	–1.5	10000	3.0	**52**	–0.5	10000	3.0	**53**	0.0	10000	3.0	**54**	+0.5	10000	3.0
	–2.5	10000	4.0		–1.5	10000	4.0		–0.5	10000	4.0		0.0	10000	4.0		+0.5	10000	4.0
	–2.5	10500	2.5		–1.5	10500	2.5		–0.5	10500	2.5		0.0	10500	2.5		+0.5	10500	2.5
55	–2.5	10500	3.5	**56**	–1.5	10500	3.5	**57**	–0.5	10500	3.5	**58**	0.0	10500	3.5	**59**	+0.5	10500	3.5
	–2.5	10500	4.0		–1.5	10500	4.0		–0.5	10500	4.0		0.0	10500	4.0		+0.5	10500	4.0
	–2.5	11000	2.5		–1.5	11000	2.5		–0.5	11000	2.5		0.0	11000	2.5		+0.5	11000	2.5
60	–2.5	11000	3.5	**61**	–1.5	11000	3.5	**62**	–0.5	11000	3.5	**63**	0.0	11000	3.5	**64**	+0.5	11000	3.5
	–2.5	11000	4.0		–1.5	11000	4.0		–0.5	11000	4.0		0.0	11000	4.0		+0.5	11000	4.0
	–2.5	11500	2.5		–1.5	11500	2.5		–0.5	11500	2.5		0.0	11500	2.5		+0.5	11500	2.5
65	–2.5	11500	3.5	**66**	–1.5	11500	3.5	**67**	–0.5	11500	3.5	**68**	0.0	11500	3.5	**69**	+0.5	11500	3.5
	–2.5	11500	4.0		–1.5	11500	4.0		–0.5	11500	4.0		0.0	11500	4.0		+0.5	11500	4.0
	–2.5	12000	2.5		–1.5	12000	2.5		–0.5	12000	2.5		0.0	12000	2.5		+0.5	12000	2.5
70	–2.5	12000	3.5	**71**	–1.5	12000	3.5	**72**	–0.5	12000	3.5	**73**	0.0	12000	3.5	**74**	+0.5	12000	3.5
	–2.5	12000	4.0		–1.5	12000	4.0		–0.5	12000	4.0		0.0	12000	4.0		+0.5	12000	4.0
	–2.5	12500	2.5		–1.5	12500	2.5		–0.5	12500	2.5		0.0	12500	2.5		+0.5	12500	2.5
75	–2.5	12500	3.5	**76**	–1.5	12500	3.5	**77**	–0.5	12500	3.5	**78**	0.0	12500	3.5	**79**	+0.5	12500	3.5
	–2.5	12500	4.0		–1.5	12500	4.0		–0.5	12500	4.0		0.0	12500	4.0		+0.5	12500	4.0
	–2.5	13000	2.5		–1.5	13000	2.5		–0.5	13000	2.5		0.0	13000	2.5		+0.5	13000	2.5
80	–2.5	13000	3.5	**81**	–1.5	13000	3.5	**82**	–0.5	13000	3.5	**83**	0.0	13000	3.5	**84**	+0.5	13000	3.5
	–2.5	13000	4.0		–1.5	13000	4.0		–0.5	13000	4.0		0.0	13000	4.0		+0.5	13000	4.0
	–2.5	13500	2.5		–1.5	13500	2.5		–0.5	13500	2.5		0.0	13500	2.5		+0.5	13500	2.5
85	–2.5	13500	3.5	**86**	–1.5	13500	3.5	**87**	–0.5	13500	3.5	**88**	0.0	13500	3.5	**89**	+0.5	13500	3.5
	–2.5	13500	4.0		–1.5	13500	4.0		–0.5	13500	4.0		0.0	13500	4.0		+0.5	13500	4.0
	–2.5	14000	2.5		–1.5	14000	2.5		–0.5	14000	2.5		0.0	14000	2.5		+0.5	14000	2.5
90	–2.5	14000	3.5	**71**	–1.5	14000	3.5	**72**	–0.5	14000	3.5	**73**	0.0	14000	3.5	**74**	+0.5	14000	3.5
	–2.5	14000	4.0		–1.5	14000	4.0		–0.5	14000	4.0		0.0	14000	4.0		+0.5	14000	4.0
	–2.5	14500	2.5		–1.5	14500	2.5		–0.5	14500	2.5		0.0	14500	2.5		+0.5	14500	2.5
95	–2.5	14500	3.5	**76**	–1.5	14500	3.5	**77**	–0.5	14500	3.5	**78**	0.0	14500	3.5	**79**	+0.5	14500	3.5
	–2.5	14500	4.0		–1.5	14500	4.0		–0.5	14500	4.0		0.0	14500	4.0		+0.5	14500	4.0
	–2.5	15000	2.5		–1.5	15000	2.5		–0.5	15000	2.5		0.0	15000	2.5		+0.5	15000	2.5
100	–2.5	15000	3.5	**101**	–1.5	15000	3.5	**102**	–0.5	15000	3.5	**103**	0.0	15000	3.5	**104**	+0.5	15000	3.5
	–2.5	15000	4.0		–1.5	15000	4.0		–0.5	15000	4.0		0.0	15000	4.0		+0.5	15000	4.0
	–2.5	15500	3.0		–1.5	15500	3.0		–0.5	15500	3.0		0.0	15500	3.0		+0.5	15500	3.0
105	–2.5	15500	3.5	**106**	–1.5	15500	3.5	**107**	–0.5	15500	3.5	**108**	0.0	15500	3.5	**109**	+0.5	15500	3.5
	–2.5	15500	4.0		–1.5	15500	4.0		–0.5	15500	4.0		0.0	15500	4.0		+0.5	15500	4.0
	–2.5	16000	3.0		–1.5	16000	3.0		–0.5	16000	3.0		0.0	16000	3.0		+0.5	16000	3.0
110	–2.5	16000	3.5	**111**	–1.5	16000	3.5	**112**	–0.5	16000	3.5	**113**	0.0	16000	3.5	**114**	+0.5	16000	3.5
	–2.5	16000	4.0		–1.5	16000	4.0		–0.5	16000	4.0		0.0	16000	4.0		+0.5	16000	4.0
	–2.5	16500	3.0		–1.5	16500	3.0		–0.5	16500	3.0		0.0	16500	3.0		+0.5	16500	3.0
115	–2.5	16500	3.5	**116**	–1.5	16500	3.5	**117**	–0.5	16500	3.5	**118**	0.0	16500	3.5	**119**	+0.5	16500	3.5
	–2.5	16500	4.0		–1.5	16500	4.0		–0.5	16500	4.0		0.0	16500	4.0		+0.5	16500	4.0

Table 1. continued

	$[Z/Z_\odot]$	T	log g		$[Z/Z_\odot]$	T	log g		$[Z/Z_\odot]$	T	log g		$[Z/Z_\odot]$	T	log g		$[Z/Z_\odot]$	T	log g
	–2.5	17000	3.0		–1.5	17000	3.0		–0.5	17000	3.0		0.0	17000	3.0		+0.5	17000	3.0
120	–2.5	17000	3.5	121	–1.5	17000	3.5	122	–0.5	17000	3.5	123	0.0	17000	3.5	124	+0.5	17000	3.5
	–2.5	17000	4.0		–1.5	17000	4.0		–0.5	17000	4.0		0.0	17000	4.0		+0.5	17000	4.0
	–2.5	17500	3.0		–1.5	17500	3.0		–0.5	17500	3.0		0.0	17500	3.0		+0.5	17500	3.0
125	–2.5	17500	3.5	126	–1.5	17500	3.5	127	–0.5	17500	3.5	128	0.0	17500	3.5	129	+0.5	17500	3.5
	–2.5	17500	4.0		–1.5	17500	4.0		–0.5	17500	4.0		0.0	17500	4.0		+0.5	17500	4.0
	–2.5	18000	3.0		–1.5	18000	3.0		–0.5	18000	3.0		0.0	18000	3.0		+0.5	18000	3.0
130	–2.5	18000	3.5	131	–1.5	18000	3.5	132	–0.5	18000	3.5	133	0.0	18000	3.5	134	+0.5	18000	3.5
	–2.5	18000	4.0		–1.5	18000	4.0		–0.5	18000	4.0		0.0	18000	4.0		+0.5	18000	4.0
	–2.5	18500	3.0		–1.5	18500	3.0		–0.5	18500	3.0		0.0	18500	3.0		+0.5	18500	3.0
135	–2.5	18500	3.5	136	–1.5	18500	3.5	137	–0.5	18500	3.5	138	0.0	18500	3.5	139	+0.5	18500	3.5
	–2.5	18500	4.0		–1.5	18500	4.0		–0.5	18500	4.0		0.0	18500	4.0		+0.5	18500	4.0
	–2.5	19000	3.0		–1.5	19000	3.0		–0.5	19000	3.0		0.0	19000	3.0		+0.5	19000	3.0
140	–2.5	19000	3.5	141	–1.5	19000	3.5	142	–0.5	19000	3.5	143	0.0	19000	3.5	144	+0.5	19000	3.5
	–2.5	19000	4.0		–1.5	19000	4.0		–0.5	19000	4.0		0.0	19000	4.0		+0.5	19000	4.0
	–2.5	19500	3.0		–1.5	19500	3.0		–0.5	19500	3.0		0.0	19500	3.0		+0.5	19500	3.0
145	–2.5	19500	3.5	146	–1.5	19500	3.5	147	–0.5	19500	3.5	148	0.0	19500	3.5	149	+0.5	19500	3.5
	–2.5	19500	4.0		–1.5	19500	4.0		–0.5	19500	4.0		0.0	19500	4.0		+0.5	19500	4.0
	–2.5	20000	3.0		–1.5	20000	3.0		–0.5	20000	3.0		0.0	20000	3.0		+0.5	20000	3.0
150	–2.5	20000	3.5	151	–1.5	20000	3.5	152	–0.5	20000	3.5	153	0.0	20000	3.5	154	+0.5	20000	3.5
	–2.5	20000	4.0		–1.5	20000	4.0		–0.5	20000	4.0		0.0	20000	4.0		+0.5	20000	4.0
	–2.5	21000	3.0		–1.5	21000	3.0		–0.5	21000	3.0		0.0	21000	3.0		+0.5	21000	3.0
155	–2.5	21000	3.5	156	–1.5	21000	3.5	157	–0.5	21000	3.5	158	0.0	21000	3.5	159	+0.5	21000	3.5
	–2.5	21000	4.0		–1.5	21000	4.0		–0.5	21000	4.0		0.0	21000	4.0		+0.5	21000	4.0
	–2.5	22000	3.0		–1.5	22000	3.0		–0.5	22000	3.0		0.0	22000	3.0		+0.5	22000	3.0
160	–2.5	22000	3.5	161	–1.5	22000	3.5	162	–0.5	22000	3.5	163	0.0	22000	3.5	164	+0.5	22000	3.5
	–2.5	22000	4.0		–1.5	22000	4.0		–0.5	22000	4.0		0.0	22000	4.0		+0.5	22000	4.0
	–2.5	23000	3.0		–1.5	23000	3.0		–0.5	23000	3.0		0.0	23000	3.0		+0.5	23000	3.0
165	–2.5	23000	3.5	166	–1.5	23000	3.5	167	–0.5	23000	3.5	168	0.0	23000	3.5	169	+0.5	23000	3.5
	–2.5	23000	4.0		–1.5	23000	4.0		–0.5	23000	4.0		0.0	23000	4.0		+0.5	23000	4.0
	–2.5	24000	3.0		–1.5	24000	3.0		–0.5	24000	3.0		0.0	24000	3.0		+0.5	24000	3.0
170	–2.5	24000	3.5	171	–1.5	24000	3.5	172	–0.5	24000	3.5	173	0.0	24000	3.5	174	+0.5	24000	3.5
	–2.5	24000	4.0		–1.5	24000	4.0		–0.5	24000	4.0		0.0	24000	4.0		+0.5	24000	4.0
	–2.5	25000	3.0		–1.5	25000	3.0		–0.5	25000	3.0		0.0	25000	3.0		+0.5	25000	3.0
175	–2.5	25000	3.5	176	–1.5	25000	3.5	177	–0.5	25000	3.5	178	0.0	25000	3.5	179	+0.5	25000	3.5
	–2.5	25000	4.0		–1.5	25000	4.0		–0.5	25000	4.0		0.0	25000	4.0		+0.5	25000	4.0
	–2.5	26000	3.0		–1.5	26000	3.0		–0.5	26000	3.0		0.0	26000	3.0		+0.5	26000	3.0 (59)
180	–2.5	26000	3.5	181	–1.5	26000	3.5	182	–0.5	26000	3.5	183	0.0	26000	3.5	184	+0.5	26000	3.5
	–2.5	26000	4.0		–1.5	26000	4.0		–0.5	26000	4.0		0.0	26000	4.0		+0.5	26000	4.0
	–2.5	27000	3.0		–1.5	27000	3.0		–0.5	27000	3.0		0.0	27000	3.0 (63)		+0.5	27000	3.0 (59)
185	–2.5	27000	3.5	186	–1.5	27000	3.5	187	–0.5	27000	3.5	188	0.0	27000	3.5	189	+0.5	27000	3.5
	–2.5	27000	4.0		–1.5	27000	4.0		–0.5	27000	4.0		0.0	27000	4.0		+0.5	27000	4.0
	–2.5	28000	3.0		–1.5	28000	3.0		–0.5	28000	3.0		0.0	28000	3.0 (54)		+0.5	28000	3.0 (57)
190	–2.5	28000	3.5	191	–1.5	28000	3.5	192	–0.5	28000	3.5	193	0.0	28000	3.5	194	+0.5	28000	3.5
	–2.5	28000	4.0		–1.5	28000	4.0		–0.5	28000	4.0		0.0	28000	4.0		+0.5	28000	4.0
	–2.5	29000	3.0		–1.5	29000	3.0		–0.5	29000	3.0 (57)		0.0	29000	3.0 (54)		+0.5	29000	3.25 (57)
195	–2.5	29000	3.5	196	–1.5	29000	3.5	197	–0.5	29000	3.5	198	0.0	29000	3.5	199	+0.5	29000	3.5
	–2.5	29000	4.0		–1.5	29000	4.0		–0.5	29000	4.0		0.0	29000	4.0		+0.5	29000	4.0
	–2.5	30000	3.25		–1.5	30000	3.25		–0.5	30000	3.25		0.0	30000	3.25 (63)		+0.5	30000	3.25 (57)
200	–2.5	30000	3.5	201	–1.5	30000	3.5	202	–0.5	30000	3.5	203	0.0	30000	3.5	204	+0.5	30000	3.5
	–2.5	30000	4.0		–1.5	30000	4.0		–0.5	30000	4.0		0.0	30000	4.0		+0.5	30000	4.0
	–2.5	31000	3.25		–1.5	31000	3.25		–0.5	31000	3.25		0.0	31000	3.25 (53)		+0.5	31000	3.25 (58)
205	–2.5	31000	3.5	206	–1.5	31000	3.5	207	–0.5	31000	3.5	208	0.0	31000	3.5	209	+0.5	31000	3.5 (58)
	–2.5	31000	4.0		–1.5	31000	4.0		–0.5	31000	4.0		0.0	31000	4.0		+0.5	31000	4.0
	–2.5	32000	3.25		–1.5	32000	3.25		–0.5	32000	3.25 (57)		0.0	32000	3.25 (53)				
210	–2.5	32000	3.5	211	–1.5	32000	3.5	212	–0.5	32000	3.5	213	0.0	32000	3.5	214	+0.5	32000	3.5 (58)
	–2.5	32000	4.0		–1.5	32000	4.0		–0.5	32000	4.0		0.0	32000	4.0		+0.5	32000	4.0
215	–2.5	33000	3.5	216	–1.5	33000	3.5	217	–0.5	33000	3.5	218	0.0	33000	3.5 (58)	219	+0.5	33000	3.5 (56)
	–2.5	33000	4.0		–1.5	33000	4.0		–0.5	33000	4.0		0.0	33000	4.0		+0.5	33000	4.0
	–2.5	34000	3.5		–1.5	34000	3.5		–0.5	34000	3.5		0.0	34000	3.5 (53)		+0.5	34000	4.0
	–2.5	34000	4.0		–1.5	34000	4.0		–0.5	34000	4.0		0.0	34000	4.0		+0.5	34000	4.5
	–2.5	35000	3.5		–1.5	35000	3.5		–0.5	35000	3.5		0.0	35000	3.5 (47)		+0.5	35000	4.0
	–2.5	35000	4.0		–1.5	35000	4.0		–0.5	35000	4.0		0.0	35000	4.0		+0.5	35000	4.5
220	–2.5	37500	4.0	221	–1.5	37500	4.0	222	–0.5	37500	4.0	223	0.0	37500	4.0	224	+0.5	37500	4.0 (56)
	–2.5	37500	4.5		–1.5	37500	4.5		–0.5	37500	4.5		0.0	37500	4.5		+0.5	37500	4.5
	–2.5	40000	4.0		–1.5	40000	4.0		–0.5	40000	4.0		0.0	40000	4.0 (55)				
	–2.5	40000	4.5		–1.5	40000	4.5		–0.5	40000	4.5		0.0	40000	4.5		+0.5	40000	4.5
	–2.5	42500	4.5		–1.5	42500	4.5		–0.5	42500	4.5		0.0	42500	4.5		+0.5	42500	4.5 (61)
	–2.5	45000	4.5		–1.5	45000	4.5		–0.5	45000	4.5		0.0	45000	4.5		+0.5	45000	4.5 (56)
	–2.5	47500	4.5		–1.5	47500	4.5		–0.5	47500	4.5		0.0	47500	4.5		+0.5	47500	4.5 (56)
	–2.5	50000	4.5		–1.5	50000	4.5		–0.5	50000	4.5		0.0	50000	4.5 (57)		+0.5	50000	4.5 (56)

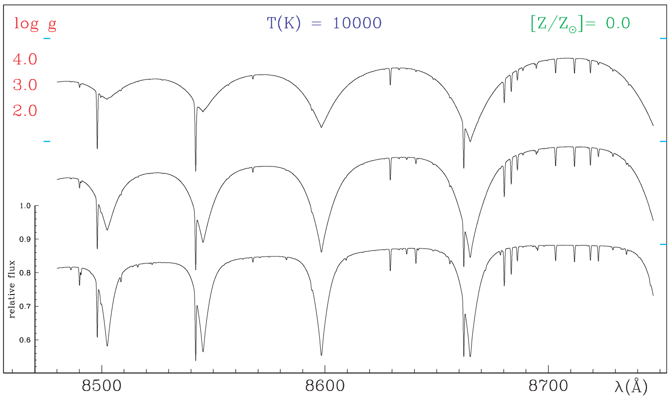

Fig. 4. A sample of $T_{\rm eff}$ = 10 000 K, $[Z/Z_\odot]$ = 0.0 synthetic spectra arranged in a sequence showing the effect of varying the gravity. The thick dashes mark the 1.00 level of the continuum. This is an example of the Figs. 5–224 available only electronically

The most relevant absorption lines in the 8490–8750 Å range are tabulated in Table 2 for $T_{\rm eff}$ = 8 000 K (log g = 2.0 and 4.0) and $T_{\rm eff}$ = 11 000 K (log g = 2.5 and 4.0), in Table 3 for $T_{\rm eff}$ = 15 000 K (log g = 2.5 and 4.0) and $T_{\rm eff}$ = 20 000 K (log g = 3.0 and 4.0), in Table 4 for $T_{\rm eff}$ = 26 000 K (log g = 3.0 and 4.0), $T_{\rm eff}$ = 33 000 K (log g = 3.5 and 4.0), and $T_{\rm eff}$ = 40 000 K (log g = 4.5).

The synthetic spectra are based on the grids of model atmospheres computed by Kurucz (1993a). Only for $T_{\rm eff}$ $\leq$ 8 750 K the models are from Castelli (1999) and differ from Kurucz's models only for the convection. Most of the models used in this paper are available at Kurucz's website (`http://kurucz.harvard.edu`). Models not available there were computed by us with the ATLAS9 code. However, some of the additional models computed for high $T_{\rm eff}$ and low gravity may be not accurate enough owing to the too small number of layers used for their computations. This shortcoming is related with the lack of line opacity data for small pressures (log $P_{\rm gas} < -2.0$) in the opacity distribution function tables we used (Kurucz 1993c–e). Because the gas pressure is very low in the uppermost layers of hot giants, the inadequate opacity gives rise to numerical problems which we have overcame by dropping the upper layers. The number of adopted layers is indicated in Table 1 in parenthesis for models computed with less than 64 optical depths, which is the minimum number of layers used in the Kurucz's grids.

The synthetic spectra were computed with the SYNTHE code of Kurucz (1993b) at a 500 000 resolving power. The spectra were degraded to the $\lambda/\Delta\lambda$ = 20 000 resolving power by adopting a Gaussian instrumental profile. The line spectrum was computed for a microturbulent velocity $\xi = 2$ km s^{-1}, while no rotational velocity and no macroturbulent velocity have been considered.

For the synthetic spectra we adopted the solar abundances given by Grevesse et al. (1996) while the model atmospheres (which are based on Kurucz' ODFs) use the Anders & Grevesse (1989) solar abundances. Elements for which the abundances in model atmospheres and synthetic spectra differ are N (–0.08) O (–0.06), F (–0.04), S (+0.09), Ar (–0.06), K (–0.12), Sc (+0.08), Ti (+0.04), Fe (–0.15), Sr (+0.07), Zr (+0.10), La (–0.05), Ce (+0.03). The numbers in parenthesis are the logarithmic differences between the abundances from Anders & Grevesse and Grevesse et al. (1996). Finally, Kurucz & Bell (1995) has been the source for the atomic lines data (see also Kurucz 1995 and the Kurucz's website).

References

Anders, E., & Grevesse, N. 1989, Geochim. Cosmochim. Acta, 53,197
Black, J. H., Wisheit, J. C., & Laviana, E. 1972, ApJ, 177, 567
Castelli, F. 1999, A&A, 346, 564
Friedrich, H., & Trefftz, E. 1969, MPI-PAE/Astro, 29
Fuhr, J. R., Martin, G. A., & Wiese, W. L. 1988., J. Phys. Chem. Ref. Data, 17, Suppl. 4
Gilmore, G., Perryman, M., Lindegren, L., et al. 1998, Proc. SPIE Conf., 3350, 541
Grevesse, N., Noels, A., & Sauval, A. J. 1996, in Cosmic Abundances, ed. S. S. Holt, & G. Sonneborn, ASP Conf. Ser., 99, ASP San Francisco, 117
Kurucz, R. L. 1988, Trans. IAU, XXB, ed. M. McNally (Kluwer), 168
Kurucz, R. L. 1993a, ATLAS9 Stellar Atmospheres Programs and 2 km s^{-1} grid, CD-ROM, No. 13
Kurucz, R. L. 1993b, SYNTHE Spectrum Synthesis Programs and Line Data, CD-ROM, No. 18
Kurucz, R. L. 1993c, Opacities for Stellar Atmospheres: [+0.0], [+0.5], [+1.0], CD-ROM No. 2
Kurucz, R. L. 1993d, Opacities for Stellar Atmospheres: [−0.5], [−1.0], [−1.5], CD-ROM No. 3
Kurucz, R. L. 1993e, Opacities for Stellar Atmospheres: [−2.0], [−2.5], [−3.0], CD-ROM No. 4
Kurucz, R. L. 1995, Astrophysical Applications of Powerful New Databases, ed. S. J. Adelman, & W. L. Wiese, ASP Conf., 78, 205
Kurucz, R. L., & Bell, B. 1995, Atomic Line List, CD-ROM, No. 23
Kurucz, R. L., & Peytremann, E. 1975, SAO Special Report, 362
McEachran, R. P., & Cohen, M. 1971, JQSRT, 11, 1819
Merat, P., Safa, F., Camus, J. P., Pace, O., & Perryman, M. A. C. 1999, in Proceedings of the ESA Leiden Workshop on GAIA, 23–27 Nov. 1998, Baltic Astron., 8, 1
Munari, U. 1999, in Proceedings of the ESA Leiden Workshop on GAIA, 23–27 Nov. 1998, Baltic Astron., 8, 73
Munari, U., & Tomasella, L. 1999, A&AS, 137, 521 (Paper I)
Munari, U., & Castelli, F. 2000, A&AS, 141, 141 (Paper II)
Murphy, P. W. 1968, JOSA, 58, 1200
Perryman, M. A. C. 1999, S&T, 97, 48
Wiese, W. L., Smith, M. W., & Glennon, B. M. 1966, NSRDS-NBS 4